COMMUNICATIONS IN NUMERICAL METHODS IN ENGINEERING
Commun. Numer. Meth. Engng 2002; **18**:711–720 (DOI: 10.1002/cnm.531)

Problems associated with the use of Cayley transform and tangent scaling for conserving energy and momenta in the Reissner–Simo beam theory

Gordan Jelenić* and Michael A. Crisfield†

Department of Aeronautics, Imperial College of Science, Technology and Medicine, London SW7 2BY, U.K.

SUMMARY

Conservation of the total energy and the total momenta in time-stepping schemes for non-linear 3D beams of the Reissner–Simo type is achieved via a particular treatment of large 3D rotations, which involves a rotational update using Cayley transformation, an interpolation of incremental tangent-scaled rotations and a non-linear update formula for angular velocities. In this note we investigate the side-effects of this procedure. Copyright © 2002 John Wiley & Sons, Ltd.

KEY WORDS: large rotations; 3D beams; strain invariance; conserving algorithms

1. INTRODUCTION

In energy/momentum-conserving time-stepping methods for non-linear elastodynamics [1–10], an algorithmic equilibrium is usually satisfied at a point within a time step rather than at the end of the time step, with the algorithmic internal load vector being defined as a function of the linear combination of the stresses at the ends of the time step, and the algorithmic inertial load vector being a difference of the momenta at the ends of the time step divided by the time step length. For some problems such as 3D solids [3] or bars [4] with the strain energy defined in terms of Green–Lagrange strains and 2nd Piola–Kirchhoff stresses, such a definition of the algorithmic equilibrium immediately provides conservation of the total translational and angular momenta of unloaded systems with pure Neumann boundary conditions. The conservation of the total energy is then provided by a specific definition of algorithmic stresses and takes a particularly straightforward form for a Saint Venant–Kirchhoff material, where it is defined as the average of the stresses at both ends of a time step.

In the presence of 3D rotation variables, a number of additional complexities are introduced which make it much more difficult to conserve the momenta and the energy, even for linear

*Correspondence to: G. Jelenić, Department of Aeronautics, Imperial College, Prince Consort Road, London SW7 2BY U.K.
†Deceased.

Contract/grant sponsor: Engineering and Physical Sciences Research Council; contract/grant number: AF/100089

Received 3 December 2001
Accepted 4 February 2002

elastic problems. In order to conserve the total energy, it is usually necessary to interpolate the *incremental* rotations [1, 5, 10] (rather than the total or iterative rotations), while in order to conserve the total energy and the total translational and angular momenta simultaneously, it has been found necessary [1, 10] to define the rotation tensor spanned by the incremental rotation using the Cayley transformation rather than the exponential mapping and to perform the update of angular velocities in terms of these incremental rotations. In order to design an energy and momentum conserving algorithm for elastic problems with 3D rotations, it was recently indicated that an alternative solution to the use of scaled rotations may be found by employing an algorithmic rate form of strain measures [7] or a different definition of the internal load vector [8].

As an additional problem, in the Reissner–Simo 3D beam theory the strain-invariant algorithms have to be specifically designed by carefully choosing a suitable interpolation for 3D rotations [5, 10–12].

In this note we examine the performance of the energy/momentum-conserving algorithm by Simo *et al.* [1] with respect to invariance properties and consider its side effects. In addition to the loss of strain invariance following a standard interpolation of 3D rotations [10–12], the loss of strain invariance is here further triggered by two distinct and not immediately obvious phenomena.

2. OUTLINE OF THE REISSNER–SIMO BEAM THEORY

We begin by summarizing the beam theory developed by Reissner, Antman and Simo and presented in References [13–15]. Wherever possible, we also use the notation employed in Reference [1]. For further details, the reader is referred to the original references.

Kinematics: For a given arc-length parameter $s \in [0, L] \subset \mathscr{R}$, $L \in \mathscr{R}$, where L is the initial length of the beam, we define a position of the beam centroid axis by a space curve $s \rightarrow \boldsymbol{\varphi} \in \mathscr{R}^3$ in a three-dimensional ambient space $\mathscr{R}^3$ with a right-handed inertial Cartesian frame $\mathbf{e}_1$, $\mathbf{e}_2$, $\mathbf{e}_3$. Cross-sections of the beam in this configuration are defined by a right-handed orthonormal triad of base vectors $s \rightarrow \mathbf{t}_1, \mathbf{t}_2, \mathbf{t}_3 \in \mathscr{R}^3$ with the base vectors $\mathbf{t}_1$ and $\mathbf{t}_2$ directed along the principal axes of inertia of the cross-section at s. The orthonormal bases $\mathbf{t}_1$, $\mathbf{t}_2$, $\mathbf{t}_3$ and $\mathbf{e}_1$, $\mathbf{e}_2$, $\mathbf{e}_3$ are related through a linear transformation $s \rightarrow \boldsymbol{\Lambda} \in \mathrm{SO}(3)$ as $\mathbf{t}_i = \boldsymbol{\Lambda}\mathbf{e}_i$, $i = 1, 2, 3$, where SO(3) is the three-parametric Lie group of proper orthogonal transformations satisfying $\det \boldsymbol{\Lambda} = 1$ and $\boldsymbol{\Lambda}\boldsymbol{\Lambda}^t = \mathbf{I}\ \forall\ s \in [0, L]$, with $\mathbf{I}$ being a 3×3 unit matrix. The position vector of the centroid axis of the beam and the orientation of the orthonormal frame attached to the cross-section at s thus fully define the current configuration of the beam $s \rightarrow \mathscr{C} = (\boldsymbol{\varphi}, \boldsymbol{\Lambda}) \in \mathscr{R}^3 \times \mathrm{SO}(3)$. In a similar manner, we define the initial configuration of the beam $s \rightarrow \mathscr{C}_0 = (\boldsymbol{\varphi}_0, \boldsymbol{\Lambda}_0) \in \mathscr{R}^3 \times \mathrm{SO}(3)$.

The velocity field of the line of centroids is given by $\mathbf{v} = \dot{\boldsymbol{\varphi}}$ and the spatial angular velocity tensor is given by $\hat{\mathbf{w}} = \dot{\boldsymbol{\Lambda}}\boldsymbol{\Lambda}^t$, with the dot representing a time derivative and the hat denoting a skew-symmetric matrix associated with the hatted quantity such that $\hat{\mathbf{a}}\mathbf{b} = \mathbf{a} \times \mathbf{b}$ for any two 3D vectors $\mathbf{a}$, $\mathbf{b}$. The material angular velocity tensor consequently follows as $\mathbf{W} = \boldsymbol{\Lambda}^t\dot{\boldsymbol{\Lambda}}$.

Equilibrium: Assume that the deformation from the initial to the deformed configuration is caused by distributed external forces and torques $\bar{\mathbf{n}}$ and $\bar{\mathbf{m}}$. The differential equilibrium equations of the beam are given as $\mathbf{n}' + \bar{\mathbf{n}} = A\rho\dot{\mathbf{v}}$ and $\mathbf{m}' + \boldsymbol{\varphi}' \times \mathbf{n} + \bar{\mathbf{m}} = \dot{\boldsymbol{\pi}}$, where $\mathbf{n}$ and $\mathbf{m}$ are the vectors of (spatial) stress and stress-couple resultants acting over the cross-section at s, A is the area of the cross-section, ρ is the initial density of the material, $\boldsymbol{\pi} = \boldsymbol{\Lambda}\mathbf{J}_\rho\mathbf{W}$ is the specific angular momentum of the cross-section with respect to its centroid, $\mathbf{J}_\rho$ is the material (time-independent) mass moment of inertia tensor of the cross-section with respect to its centroid and the prime ($'$) denotes a differentiation with respect to the arc-length parameter s.

Strains and constitutive relationship: The strain-configuration relations are given as

$$\boldsymbol{\Gamma} = \boldsymbol{\Lambda}^t \boldsymbol{\varphi}' - \boldsymbol{\Lambda}_0^t \boldsymbol{\varphi}_0' \quad \text{and} \quad \hat{\boldsymbol{\Omega}} = \boldsymbol{\Lambda}^t \boldsymbol{\Lambda}' - \boldsymbol{\Lambda}_0^t \boldsymbol{\Lambda}_0'$$

where $\boldsymbol{\Gamma}$ and $\boldsymbol{\Omega}$ are (material) translational and rotational strain measures, which are energy-conjugate to the (material) stress and stress-couple resultants $\mathbf{N} = \boldsymbol{\Lambda}^t \mathbf{n}$ and $\mathbf{M} = \boldsymbol{\Lambda}^t \mathbf{m}$. In the case of a linear elastic material, the relationships between the stress/stress-couple resultants and the adopted strain measures are defined as $\mathbf{N} = \mathbf{C}_N \boldsymbol{\Gamma}$ and $\mathbf{M} = \mathbf{C}_M \boldsymbol{\Omega}$ with $\mathbf{C}_N = \mathrm{diag}(GA_1, GA_2, EA)$ and $\mathbf{C}_M = \mathrm{diag}(EI_1, EI_2, GI_t)$ as constant constitutive tensors. Here E and G denote Young's and the shear moduli, A_1 and A_2 are the shear areas, I_1 and I_2 are the second moment of areas with respect to base vectors $\mathbf{t}_1$ and $\mathbf{t}_2$ and I_t is the torsional constant of the cross-section.

3. BRIEF OUTLINE OF THE ALGORITHM (1)

The crucial result of Simo *et al.* [1] can be summarized as follows. The implicit time-stepping algorithm for the non-linear dynamics of 3D Reissner–Simo beams, which conserves by definition the total energy of a Hamiltonian system and the total translational and angular momenta of the system in the absence of applied loads and reactions is defined by the following dynamic nodal residual vector:

$$\mathbf{R}^A = \mathbf{F}_{\mathrm{int}}^A - \mathbf{F}_{\mathrm{ext}}^A = \mathbf{0} \quad \text{for } A = 1, \ldots, N_{\mathrm{node}} \tag{1}$$

where N_{node} is the number of nodes on the beam finite element, $\mathbf{F}_{\mathrm{ext}}^A$ is the nodal vector of applied (conservative) loads and $\mathbf{F}_{\mathrm{int}}^A$ is the nodal vector of elastic and inertial contributions. This vector is defined by Equation (95) in Reference [1] as

$$\mathbf{F}_{\mathrm{int}}^A = \int_0^L \left(\begin{bmatrix} N^{A'}\mathbf{I} & \mathbf{0} \\ -N^A \hat{\boldsymbol{\varphi}}_{n+1/2}' & N^{A'}\mathbf{I} \end{bmatrix} \begin{Bmatrix} \boldsymbol{\Lambda}_{n+1/2}\mathbf{N}_{n+\alpha} \\ \boldsymbol{\Lambda}_{n+1/2}^* \mathbf{M}_{n+\alpha} \end{Bmatrix} + \frac{N^A}{\Delta t} \begin{Bmatrix} A\rho(\mathbf{v}_{n+1} - \mathbf{v}_n) \\ \pi_{n+1} - \pi_n \end{Bmatrix} \right) \mathrm{d}s \tag{2}$$

where $N^B(s)$ are standard Lagrangian interpolation functions for $B = 1, \ldots, N_{\mathrm{node}}$, Δt is the time-step length, the indices n and $n+1$ denote that the quantity in question is to be evaluated at times t_n and t_{n+1}, respectively, and the index $n+\alpha$ indicates that a quantity $(\bullet)$ is to be evaluated using $(\bullet)_{n+\alpha} = (1-\alpha)(\bullet)_n + \alpha(\bullet)_{n+1}$. For a linear elastic material, $\alpha = \frac{1}{2}$. Finally, $\boldsymbol{\Lambda}_{n+1/2}^*$ is defined as $\boldsymbol{\Lambda}_{n+1/2}^* = \det(\boldsymbol{\Lambda}_{n+1/2})\boldsymbol{\Lambda}_{n+1/2}^{-t}$. This result has to be supplemented with time-advancing formulae (37) in Reference [1] of the type

$$\frac{\boldsymbol{\varphi}_{n+1} - \boldsymbol{\varphi}_n}{\Delta t} = \mathbf{v}_{n+1/2} \quad \text{and} \quad \frac{\boldsymbol{\Theta}}{\Delta t} = \mathbf{W}_{n+1/2} \tag{3}$$

with $\boldsymbol{\Lambda}_{n+1} = \boldsymbol{\Lambda}_n \mathrm{cay}\boldsymbol{\Theta}$ and $\mathrm{cay}\boldsymbol{\Theta} = \mathbf{I} + 1/(1 + (1/4)\Theta)(\hat{\boldsymbol{\Theta}} + \frac{1}{2}\hat{\boldsymbol{\Theta}}^2)$ for an *algorithmic* incremental material rotation $\boldsymbol{\Theta}$ with the norm $\Theta = \|\boldsymbol{\Theta}\|$, and with interpolation of the (spatial) *algorithmic* *incremental rotation* between configurations at times t_n and t_{n+1}, $\boldsymbol{\vartheta} = \boldsymbol{\Lambda}\boldsymbol{\Theta}$, of the type

$$\boldsymbol{\vartheta}(s) \doteq \sum_{A=1}^{N_{\text{node}}} N^A(s)\boldsymbol{\vartheta}_A \tag{4}$$

given by Equation $(88\text{a})_2$ in Reference [1]. For the sake of completeness, let us mention that the interpolation of the incremental displacements is performed in the standard way using $\boldsymbol{\varphi}_{n+1}(s) - \boldsymbol{\varphi}_n(s) \doteq \sum_{A=1}^{N_{\text{node}}} N^A(s)(\boldsymbol{\varphi}_{n+1,A} - \boldsymbol{\varphi}_{n,A})$.

Discussion of the algorithm [1]: There are two inherent features of the above algorithm:

(i) The property of Algorithm [1] to simultaneously conserve both the total energy and the total momenta is inextricably connected to the interpolation of rotations (4). From the relationship $\boldsymbol{\Lambda}_{n+1} = \operatorname{cay}\boldsymbol{\vartheta}\boldsymbol{\Lambda}_n = \exp\hat{\boldsymbol{\psi}}\boldsymbol{\Lambda}_n \Leftrightarrow \boldsymbol{\vartheta} = (\tan(\psi/2)/(\psi/2))\boldsymbol{\psi}$, $\psi = \|\boldsymbol{\psi}\|$, we see that the quantity interpolated by Equation (4) is not the *real* incremental rotation $\boldsymbol{\psi}$, but the *algorithmic* incremental rotation $\boldsymbol{\vartheta}$, i.e. the *tangent-scaled* incremental rotation. Hence

Simultaneous conservation of energy and momenta requires interpolation of incremental tangent-scaled rotations.

Interpolation of the *unscaled* rotations, in particular, fails to provide the simultaneous conservation of energy and momenta [10], unless alternative techniques involving a re-definition of strain measures using an algorithmic rate form [7] or a re-definition of algorithmic stress resultants [8] with a possible side-effect on the order of accuracy of the solution, are employed.

(ii) In a similar vein, but related to temporal discretization, the angular velocity update formula $(3)_2$ states that

The magnitude of the algorithmic mid-point angular velocity is not defined by the angle traversed over a time step divided by the time-step length.

Instead, it is the *tangent-scaled* incremental rotation that divided by the time step length defines the magnitude of the algorithmic angular velocity.

These two characteristic features of Algorithm [1] impose important consequences on the solution. In order to investigate them, in the following section we present a test example for which a closed-form solution is available.

4. A SIMPLE DYNAMICALLY STRAIN-INVARIANT PROBLEM—ANALYTICAL SOLUTION

To reach conclusions about the invariance properties of a static formulation it would be sufficient to compare the strains at any two configurations, which differed from each other by a rigid-body translation and a rigid-body rotation (see, for example Reference [11]). As the rigid-body motion is not strain-producing, invariant formulations would have to provide identical strain states in the two configurations. In dynamics, however, the mere application of a rigid body motion to an elastic, dynamically active, body is a strain-producing phenomenon, so it is impossible to justify the general static concept of strain invariance. However, due to kinematic assumptions, specific to some structural models like bars, beams and shells, there exist cases where a rigid body motion may be applied without affecting the strain state in the system. One such case is plotted in Figure 1 and is taken for further analysis.

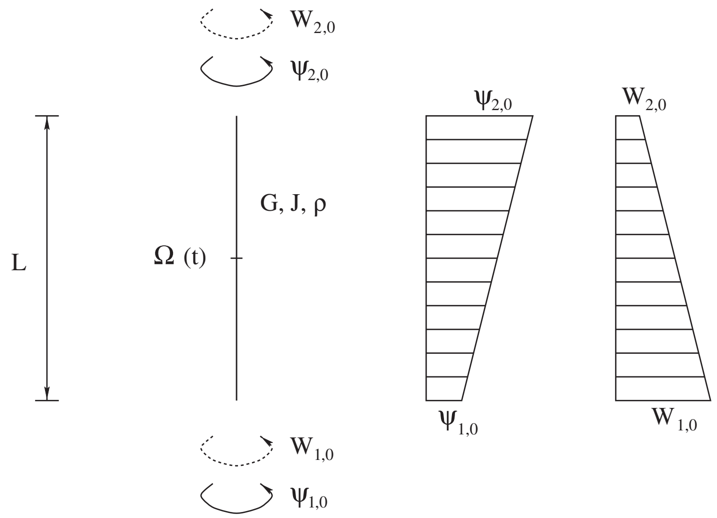

Figure 1. Uniform rod subject to initial rotations and angular velocities at each end.

In this problem, a rod of length L and uniform cross-sectional mass moment of inertia $J\rho$ and shear modulus G is floating in space due to the imposition of initial axial (i.e. torsional) rotations $\psi_{1,0}$ and $\psi_{2,0}$ and axial angular velocities $W_{1,0}$ and $W_{2,0}$ at its ends. These quantities vary linearly along the length of the rod. In this problem the curvature (torsional strain) in the middle of the rod Ω can be computed exactly as

$$\Omega(t) = \frac{4}{\pi L} \sum_{n=1,3,5,\dots}^{\infty} (-1)^{(n+3/2)} \frac{1}{n} \left[(\psi_{2,0} - \psi_{1,0}) \cos k_n t + \frac{W_{2,0} - W_{1,0}}{k_n} \sin k_n t \right]$$

where $k_n = (n\pi/L)\sqrt{G/\rho}$. This result follows from exactly integrating the differential equation of the problem $(\partial^2\psi/\partial t^2) - (G/\rho)(\partial^2\psi/\partial x^2) = 0$ for given initial conditions $t=0: \psi_0(x) = ((L-x)/L)\psi_{1,0} + (x/L)\psi_{2,0}$ and $t=0: W_0(x) = ((L-x)/L)W_{1,0} + (x/L)W_{2,0}$ and taking the first derivative of the result with respect to x. Obviously, the result is invariant to the variation of the initial parameters provided $\psi_{2,0} - \psi_{1,0} = \text{const.}$ and $W_{2,0} - W_{1,0} = \text{const.}$ It must be emphasized that this strain-invariance exists only for the adopted beam theory, which regards cross-sections as rigid and thus neglects the centrifugal and Coriolis effects that would otherwise naturally occur in a 3D continuum. At $t=0$ we have $\Omega_0 = (4/\pi L)(\psi_{2,0} - \psi_{1,0})\sum_{n=1,3,5,\dots}^{\infty}(1/n)(-1)^{(n+3)/2} = (1/L)(\psi_{2,0} - \psi_{1,0})$, i.e. the *static* solution for the curvature in the middle of the rod is invariant to the variation in end rotations $\psi_{1,0}$ and $\psi_{2,0}$ so long as $\psi_{2,0} - \psi_{1,0} = \text{const.}$

5. SOLUTION TO THE SIMPLE DYNAMICALLY STRAIN-INVARIANT PROBLEM USING ALGORITHM (1)

We will now analyse the problem given in Section 4 by applying Algorithm (1). We will model the problem by choosing only one finite element with a linear interpolation of the incremental tangent-scaled axial rotation using Equation (4). The linear element requires only one integration point for the computation of the elastic load vector (first integrand in Equation (2)), and two integration points for the computation of the inertial load vector (second integrand in Equation (2)). In order to eliminate the phenomena which are not of primary interest for the current analysis, we will perform the integration of the inertial load vector by applying two-point Newton–Cotes (or Lobatto) integration (this effectively means that the mass moments of inertia are regarded as being concentrated at the two ends of the element). In this way, the residual vector follows from Equations (1) and (2) evaluated at both nodes (note that we are left with only the axial component of the elastic and the inertial moment at each node) as

$$DGJ\,\frac{\Omega_n+\Omega_{n+1}}{2}\begin{Bmatrix}-1\\1\end{Bmatrix}+\frac{\rho JL}{2\Delta t}\begin{Bmatrix}W_{1,n+1}-W_{1,n}\\W_{2,n+1}-W_{2,n}\end{Bmatrix}=\begin{Bmatrix}0\\0\end{Bmatrix}$$

with $D=\det(\mathbf{\Lambda}_{n+1/2})=1/(1+1/16(\vartheta_1+\vartheta_2)^2)$. After applying the angular velocity update $(3)_2$, the discretised vector equation of motion becomes

$$D(\Omega_n+\Omega_{n+1})\begin{Bmatrix}-1\\1\end{Bmatrix}+\frac{2\rho L}{G\Delta t}\begin{Bmatrix}\dfrac{\vartheta_1}{\Delta t}-W_{1,n}\\[2ex]\dfrac{\vartheta_2}{\Delta t}-W_{2,n}\end{Bmatrix}=\begin{Bmatrix}0\\0\end{Bmatrix} \tag{5}$$

By realizing that the incremental curvature is $\mathbf{\Omega}_{n+1}-\mathbf{\Omega}_n=1/(1+(1/4)\vartheta^2)\mathbf{\Lambda}_n^t(\mathbf{I}-(\frac{1}{2})\hat{\boldsymbol{\vartheta}})\boldsymbol{\vartheta}'$ (this follows from Equations $(20)_2$, (39) and $(43)_1$ in Reference [1]) we obtain the incremental torsional curvature in the middle of the rod as

$$\Omega_{n+1}-\Omega_n=\frac{D}{L}(\vartheta_2-\vartheta_1) \tag{6}$$

Subtracting the first component from the second in Equation (5) gives

$$\Omega_n+\Omega_{n+1}+\frac{\rho L^2}{GD^2}\frac{1}{\Delta t^2}(\Omega_{n+1}-\Omega_n)=\frac{\rho L}{GD}\frac{1}{\Delta t}(W_{2,n}-W_{1,n}) \tag{7}$$

Equations (6) and (7) provide the following expressions for the curvature in the middle of the rod at times $t_0=0$ and $t_1=\Delta t$:

$$\Omega_0=\frac{2}{L}\,\frac{\tan\dfrac{\psi_{2,0}}{2}-\tan\dfrac{\psi_{1,0}}{2}}{1+\dfrac{1}{4}\left(\tan\dfrac{\psi_{1,0}}{2}+\tan\dfrac{\psi_{2,0}}{2}\right)^2} \tag{8}$$

$$\Omega_1=\frac{1}{1+\dfrac{\rho L^2}{GD^2\Delta t^2}}\left[\left(-1+\frac{\rho L^2}{GD^2\Delta t^2}\right)\Omega_0+\frac{\rho L}{GD\Delta t}(W_{2,0}-W_{1,0})\right] \tag{9}$$

These equations immediately reveal that (i) the solution for the torsional strain at the beginning of the first step, Ω_0, is not a function of only $\psi_{2,0}-\psi_{1,0}$ and (ii) the solution for the torsional strain at the end of the first step, Ω_1, is not a function of only $\psi_{2,0}-\psi_{1,0}$ and $W_{2,0}-W_{1,0}$.

6. DISCUSSION OF THE NUMERICAL SOLUTION TO THE SIMPLE DYNAMICALLY STRAIN-INVARIANT PROBLEM USING ALGORITHM (1)

The following conclusions can be drawn from the numerical solution for curvature in the middle of the rod at times $t=0$ and $t=\Delta t$, provided by Equations (8) and (9):

1. The algorithm suffers from the lack of strain-invariance irrespective of the time-stepping procedure. Equation (8) shows that at the beginning of the procedure,

$$t=0: \quad \Omega_0(\psi_{1,0},\psi_{2,0}) \neq \Omega_0(\psi_{1,0}+\bar{\psi},\psi_{2,0}+\bar{\psi}) \quad \text{for } \psi_{1,0}\neq\psi_{2,0} \quad \text{and} \quad \bar{\psi}\neq 0$$

   i.e. an application of a *rigid-body rotation* $\bar{\psi}$ is strain producing. This anomaly, which we will here call the *static* loss of strain-invariance is a consequence of the applied interpolation of tangent-scaled rotations (4) and is not related to the recently reported strain-invariance problems in interpolating 3D rotations [11, 12]. In contrast to the latter, the current loss of strain invariance takes place even for 2D or indeed, as is the case in the present example, for 1D problems.

   If *unscaled* incremental rotations, $\boldsymbol{\psi}$ from $\boldsymbol{\Lambda}_{n+1}=\exp\hat{\boldsymbol{\psi}}\boldsymbol{\Lambda}_n$, were interpolated, the incremental curvature would follow from $\boldsymbol{\Omega}_{n+1}-\boldsymbol{\Omega}_n=\boldsymbol{\Lambda}_n^t(\mathbf{I}-((1-\cos\psi)/\psi^2)\hat{\boldsymbol{\psi}}+((\psi-\sin\psi)/\psi^3)\hat{\boldsymbol{\psi}}^2)\boldsymbol{\psi}'$, for the present simple example ending in $\Omega_{n+1}-\Omega_n=(1/L)(\psi_2-\psi_1)$ and $\Omega_0=(1/L)(\psi_{2,0}-\psi_{1,0})$. This interpolation, however, would have an adverse effect on the conservation properties of the algorithm (see Reference [10]).

   Without going into the rather cumbersome details [5, 10], we state that the static loss of strain invariance can be rectified by providing a *configuration-dependent* interpolation of the incremental tangent-scaled rotations, while retaining all the conservation properties of the underlying algorithm. The configuration-dependent interpolation alone, however, is unable to provide the solution to the following problem.

2. By setting $\psi_{1,0}=\psi_{2,0}$ we can eliminate the static loss of strain invariance and isolate another source of the loss of strain invariance, which is caused both by the applied interpolation (4) and by the update of angular velocities (3). In this case the curvature in the middle of the rod at the end of the first time step follows from Equation (9) as

$$\Omega_1 = \frac{\dfrac{\rho L}{GD\Delta t}}{1+\dfrac{\rho L^2}{GD^2\Delta t^2}}(W_{2,0}-W_{1,0}), \quad D=\frac{1}{1+\frac{1}{16}(\vartheta_1+\vartheta_2)^2}$$

   i.e. the curvature becomes a function of the average incremental tangent-scaled rotation $\frac{1}{2}(\vartheta_1+\vartheta_2)$. This effect vanishes for $(\rho/G)\to 0$ and we will accordingly call it the *dynamic* loss of strain invariance.

   To make the point clearer, we run the example given in Section 4 with $\psi_{1,0}=\psi_{2,0}=0$ for the values of input parameters as given in Figure 2. In the first run the rod is subject only to an initial axial angular velocity $W_{2,0}$, while in the second run it is subject to initial

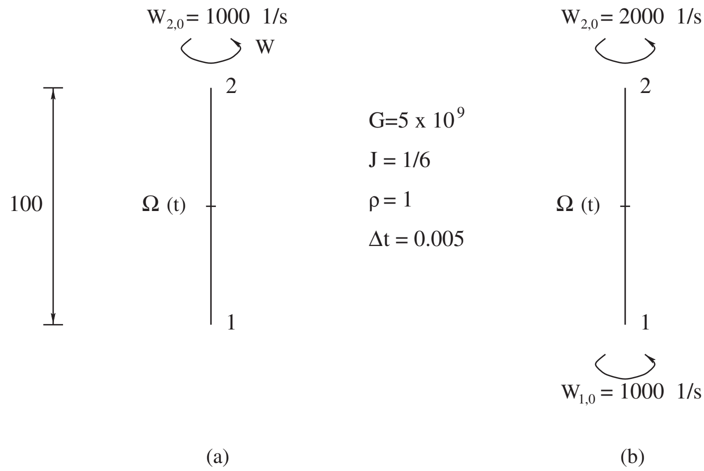

Figure 2. Unsupported rod subject to initial axial angular velocities: (a) only at node 2, (b) at both nodes.

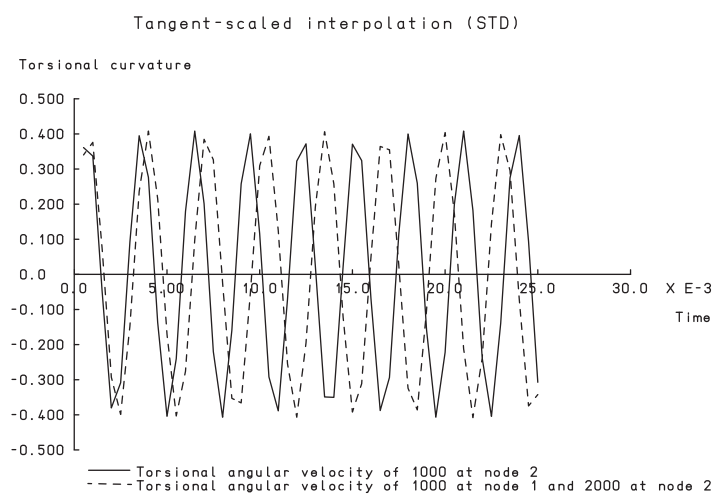

Figure 3. Algorithm (1): Torsional curvature in the centre of the rod in Figure 2: initial contitions (a) (solid line), initial conditions (b) (dashed line).

axial angular velocities $W_{1,0}$ and $W_{2,0}$ such that $W_{2,0} - W_{1,0}$ is equal to the axial angular velocity $W_{2,0}$ from the first run. As shown in Section 4, the torsional curvature in the centre of the rod should in both cases be the same. The iterative process is terminated when the square root of the sum of the squares of the nodal iterative rotations as percentage of the square root of the sum of the squares of the total nodal rotations is less than 10^{-5}. Figure 3 plots the torsional curvature against the response time in the two runs.

If unscaled incremental rotations were interpolated *and* used to update the angular velocities, there would be no loss of dynamic strain invariance, but this would have a detrimental effect on the conservation properties of the algorithm (see Reference [10]). Use of the scaling in either of the two places is enough to trigger the loss of dynamic strain invariance and in contrast to the loss of static strain invariance, experimenting with configuration-dependent tangent-scaled interpolation has yielded no solution [10].

It was shown in Reference [16] that, for this simple example, there does in fact exist a solution to the problem, which takes advantage of the fact that the original algorithm leaves the possibility to apply a certain additional scaling while performing the update of angular velocities without compromising its conservation properties. The details are again rather involved and we feel that the exceedingly limited application of the technique does not justify the space needed to present them.

7. CONCLUSIONS

In this paper, the invariance properties of an energy and momentum conserving algorithm for 3D beams with large rotations [1] have been investigated. It was shown that the loss of strain-invariance in the algorithm is a consequence of using tangent-scaled incremental rotations in the interpolation and in the update of the angular velocities.

ACKNOWLEDGEMENTS

The research was sponsored by Engineering and Physical Sciences Research Council under Advanced Research Fellowship AF/100089. The support is gratefully acknowledged.

REFERENCES

1. Simo JC, Tarnow N, Doblare M. Nonlinear dynamics of three-dimensional rods: exact energy and momentum conserving algorithms. *International Journal for Numerical Methods in Engineering* 1995; **38**:1431–1473.
2. Simo JC, Wong KK. Unconditionally stable algorithms for rigid body dynamics that exactly preserve energy and momentum. *International Journal for Numerical Methods in Engineering* 1991; **31**:19–52.
3. Simo JC, Tarnow N. The discrete energy-momentum method. Conserving algorithms for nonlinear elastodynamics. *Journal of Applied Mathematics and Physics* (ZAMP) 1992; **43**:757–792.
4. Crisfield MA, Shi J. A co-rotational element/time-integration strategy for non-linear dynamics. *International Journal for Numerical Methods in Engineering* 1994; **37**:1897–1913.
5. Crisfield MA, Jelenić G. An invariant energy-momentum conserving procedure for dynamics of 3D beams. *Proceedings of the 4th World Congress on Computational Mechanics—New Trends and Applications*, Idelsohn SR *et al*. (eds), CD ROM, Part II, Section 5, Buenos Aires, Argentina 29 June–2 July 1998. CIMNE: Barcelona, Spain.
6. Simo JC, Gonzalez O. Recent results on the numerical integration of infinite-dimensional Hamiltonian systems. In *Recent Developments in Finite Element Analysis—A Book Dedicated to Robert L. Taylor*, Hughes TJR *et al*. (eds). CIMNE: Barcelona, 1994; 255–271.
7. Sansour C, Wriggers P, Sansour J. Nonlinear dynamics of shells: Theory, finite element formulation and integration schemes. *Nonlinear Dynamics* 1997; **13**:279–305.
8. Crisfield MA, Jelenić G. Energy/momentum conserving time integration procedure with finite elements and large rotations. *Proceedings of the Advanced Research Workshop Computational Aspects of Nonlinear Structural Systems with Large Rigid Body Motion*, Ambrósio JAC, Kleiber M (eds). Pułtusk: Poland, 2–7 July 2000; 181–200.
9. Greenspan D. Completely conservative, covariant numerical methodology. *Computers and Mathematics with Applications* 1995; **29**:37–43.
10. Jelenić G. Energy–momentum dynamic integrator for geometrically exact 3D beams: Attempt at a strain-invariant solution. *Aero Report 99-04*, Department of Aeronautics. Imperial College, London, Great Britain.

11. Crisfield MA, Jelenić G. Objectivity of strain measures in geometrically exact 3D beam theory and its finite element implementation, Proceedings of the Royal Society, London Series A 1999; **455**:1125–1147.
12. Jelenić G, Crisfield MA. Geometrically exact 3D beam theory: Implementation of a strain-invariant finite element for statics and dynamics. *Computer Methods in Applied Mechanics and Engineering* 1999; **171**:141–171.
13. Reissner E. On finite deformations of space-curved beams. *Journal of Applied Mathematics and Physics* (ZAMP) 1981; **32**:734–744.
14. Antman SS. Kirchhoff's problem for nonlinearly elastic rods. *The Quarterly Journal of Applied Mathematics* 1974; **32**:221–240.
15. Simo JC. A finite strain beam formulation. The three-dimensional dynamic problem. Part I. *Computer Methods in Applied Mechanics and Engineering* 1985; **49**:55–70.
16. Jelenić G. Strain-invariance in conserving dynamic integrators for flexible systems with 3D rotations. *Extended Abstracts for the 8th Annual Conference of the Association for Computational Mechanics in Engineering*, Cross M (ed.). University of Greenwich: London, Great Britain, April 2000; 20–23.

